2008 20th International Lightning Detection Conference
21-23 April • Tucson, Arizona, USA
2nd International Lightning Meteorology Conference
24-25 April • Tucson, Arizona, USA

AN EMPIRICAL LIGHTNING CESSATION FORECAST SCHEME AT THE CAPE CANAVERAL AIR STATION AND THE KENNEDY SPACE CENTER

Geoffrey T. Stano*, Henry E. Fuelberg
Florida State University, Tallahassee, FL, USA

William P. Roeder
45th Weather Squadron, Patrick AFB, FL, USA

1. INTRODUCTION

This research addresses a seldom studied aspect of lightning—lightning cessation. Holle et al. (1992) found that the majority of casualties occur either during thunderstorm initiation or during dissipation. Between these times, when the threat of lightning is obvious, there are fewer casualties. Thus, the initiation and cessation of lightning activity are critically important periods.

Florida is particularly at risk from lightning. Florida annually receives more CG lightning than any other state (Fig. 1), earning the title "lightning capital of the United States" (Orville 1994; Hodanish et al. 1997; Orville and Huffines 2001; and Orville et al. 2002). Florida also has the most casualties of any state (Curran et al. 2000). The majority of these casualties occur during the warm season months of May through September, the climatological peak of lightning activity.

Florida's "lightning alley" is located in the central portion of the peninsula (Fig. 1), coinciding with the location of Cape Canavaerl Air Force Station (CCAFS) and Kennedy Space Center (KSC). CCAFS/KSC typically experiences four to ten CG lightning strikes per square kilometer per year (Fig. 2). Considering that CCAFS/KSC employs over 25,000 individuals, many of whom work outdoors, and has over $20 billion of facilities (Boyd et al. 1995), safety concerns require accurate forecasts of both lightning initiation and cessation. While bringing people indoors in a timely matter is important, safety is not fully met unless the advisories are left in effect through the end of lightning activity. Safety is still met if the advisory is left in effect too long, but this detracts from efficiency, impacting CCAFS/KSC both financial and in terms of the launch schedule. This has resulted in the creation of a unique lightning advisory system for the KSC region (Weems et al. 2001; Bott and Eisenhawer 2005).

*Corresponding author address: Geoffrey Stano, National Space Science and Technology Center, ENSCO, Inc., 320 Sparkman Dr., Room 3023, Huntsville, AL, 35805. Email: geoffrey.stano@nasa.gov

The 45th Weather Squadron (45WS) issues advisories that alert KSC personnel to the onset of lightning activity and signal when the threat has passed. The 45WS is reasonably satisfied with the accuracy of their lightning initiation advisories. The primary concern is when to discontinue an advisory. Previous reviews of the 45WS's lightning advisories have revealed that most are maintained too long. However, with an improved understanding of lightning cessation, the 45WS hopes that forecast guidance can be developed to assess with a high degree of confidence, whether a particular flash will be the last flash of a given thunderstorm. This, in turn, can lead to shortened, but safe advisory periods. The reduction in lost manpower hours will produce a major cost savings, estimated to be millions of dollars per year (Roeder and Glover, 2005).

Only three previous cessation studies have been conducted and all focused on the last CG strike. Hinson (1997) and Holmes (2000) utilized radar data to study thunderstorms in the KSC region, examining 3 and 40, storms respectively. Hinson found a lag time of ~30 min between the 45 dBZ reflectivity at the -10ºC level and the last CG strike. Holmes concluded that single cell and multicell thunderstorms had different cessation behaviors, with the most forecast skill found in single cells. Finally, Roeder and Glover (2005) conducted a proof of concept study on 58 thunderstorms where the inter-strike times were fit to a log-linear curve that explained 75% of the variation. They concluded that a statistical approach to forecasting lightning cessation showed promise.

This paper expands on previous cessation studies by including data from, KSC's Lightning Detection and Ranging (LDAR) network. Instead of only studying CG strikes, we consider total lightning, both CG strikes and intracloud (IC) flashes. A total of 116 storms at Cape Canaveral, Florida during the warm seasons (May-September) of 2000-2005 are analyzed. Lightning cessation characteristics are described first. Then, 100 of the storms are used to create empirical forecast

guidance that is tested on the remaining 16 storms.

2. OBSERVATION NETWORKS

2.1 Lightning Detection and Ranging

The LDAR network at KSC (Lennon 1975; Poehler and Lennon 1979; Maier et al. 1995; Britt et al. 1998; Boccippio et al. 2001) detects most IC flashes and the upper portions of CG strikes. Without the intra-cloud lightning data, this research would only be an in-depth repetition of the Roeder and Glover (2005) study. LDAR's detection efficiency is ~ 97%, increasing to 99% when events occur within 25 km of the center of the LDAR network. These findings have been confirmed by Maier et al. (1995) and Murphy et al. (2000). LDAR has a typical detection range of 100 km (Boccippio et al. 2001).

The LDAR network is a short-baseline system utilizing a Time of Arrival (TOA) detection scheme. Originally designed by NASA, the network consists of seven sensors arranged in a hexagonal pattern. Each sensor is located 6-10 km away from the controlling central receiving sensor in the middle of the network (Fig. 3). LDAR is a passive observing system (Maier et al. 1995) that operates at 66 MHz and a bandwidth of 6 MHz, sensing the VHF electromagnetic pulses generated by the individual stepped leaders, or sparks, of each lightning flash.

2.2 Cloud-to-Ground Lightning Surveillance System

KSC's Cloud-to-Ground Lightning Surveillance System (CGLSS) (Roeder et al. 2005; Boyd et al. 2005) is a high-performance, local CG lightning detector consisting of six Improved Accuracy via Combined Technology sensors (Cummins et al. 1998), similar to the National Lightning Detection Network (NLDN) (Cummins et al. 1998; 1999) (Fig. 3). CGLSS has greater detection efficiency and location accuracy than NLDN due to its greater density of sensors (Boyd et al. 2005). CGLSS has a 98% detection efficiency and 250 m location accuracy (Roeder et al. 2000).

2.3 Melbourne, FL WSR-88D Doppler Radar

The three previous lightning cessation studies (Hinson 1997; Holmes 2000; Roeder and Glover 2005) utilized radar products but only cloud-to-ground lightning data, not the total lightning data of LDAR. We used WSR-88D radar data from the National Weather Service Forecast Office in Melbourne, Florida to accurately determine the locations of isolated thunderstorms (Fig. 3, square). This allowed us to associate each lightning flash with its parent storm and to capture the full lifecycle of each storm. The Melbourne radar is located 1.13 km west and 47.32 km south of the central LDAR receiver (Hinson 1997; Holmes 2000).

2.4 Cape Canaveral Radiosondes

We also used morning radiosonde soundings from Cape Canaveral (XMR). Various wind, moisture, and stability parameters were calculated from the soundings and then used to determine if there was a statistical correlation between these parameters and lightning cessation.

Only the morning XMR soundings between 1000 and 1500 UTC were utilized since they better represent the atmosphere prior to thunderstorm initiation and contain less convective contamination. This decision is consistent with several previous studies (Neumann and Nicholson 1972; Lopez et al. 1984; Livingston et al. 1996; Brenner 2004; Shafer and Fuelberg 2006).

3. METHODOLOGIES

Our domain (Fig. 3) was confined to within 100 km of the center of the LDAR network, with preference given to storms within 60 km (inner ring, Fig. 3). This area corresponds to the most accurate regions of our observation networks, particularly LDAR. The majority of storms selected were within 60 km, although a few started or ended just outside of this distance. No storms were selected farther than 100 km.

The storms were selected using radar and lightning information. The lightning information was processed using two algorithms from the 45WS. These algorithms combined the raw LDAR sparks into flashes (Nelson 2002) and then combined the flashes with CG strikes (McNamara 2002). The lightning and radar data were visualized with the Warning Decision Support System – Integrated Information (WDSS-II) software (Lakshmanan et al. 2006). Figure 4 shows the capabilities of the WDSS-II software in this regard.

Storm selection was the most critical component of the research. Our goal was to pick storms whose lightning flashes were clearly associated with that storm. Thus, the final flash of a storm could be determined with certainty.

Although the storm selection process was subjective, it was based on several guidelines to ensure consistency. During storm selection, only the initiation point of an LDAR flash was displayed with the radar data. These initiation points were most closely related spatially with a thunderstorm's core, and removing the remaining sparks eliminated hundreds of remaining sparks that

produced clutter (Fig. 4). The initiation points had to coincide with the radar-observed location of a storm. Most lightning in active storms was located near the storm's core (i.e., greatest dBZ values), while weaker or weakening thunderstorms had more lightning dispersed throughout the cell.

All selected storms had to be isolated from one another. Without this isolation, there was no certainty that the final flash of a particular storm had been observed. This need for isolation had ramifications. First, it limited the number of storms chosen. Second, in many cases, several cells were in close proximity or would merge, preventing us from determining which flashes were associated with which storm. This forced us to pick storms that were spatially isolated, which sometimes were shorter lived and less electrically active.

Various parameters were calculated for the 116 selected storms. They included sounding-derived values of CAPE and the freezing layer, radar parameters such as the maximum height of the maximum dBZ, the total number of CG strikes, and LDAR characteristics describing the average inter-flash time and the time between the last CG strike and last IC flash. A total of 100 possible predictors were calculated (not shown).

Each possible predictor had to be screened for co-linearity. This involved a forward stepwise regression. For possible predictors that were highly correlated with one another, the predictor with the highest correlation to our predictand was selected. This process reduced our list of predictors to 33 (Table 1).

These 33 predictors were further reduced if a possible predictor could not be observed in real time, since the goal is to create an operational tool for 45WS. This eliminated several LDAR parameters, such as the average inter-flash time, since the flash creation algorithm could not be run in real time. As a result, raw LDAR data, such as the number of sparks above 10 km were used instead of the LDAR flash characteristics. These non real time LDAR parameters were retained for use in one of the experimental regressions to how our results would change if the parameters were available.

A predictand related to lightning cessation had to be chosen. We wanted to determine the amount of time to wait after a flash had occurred to know with certainty that it was the last lightning activity of the storm. The quantity maximum interval was chosen. It is the greatest time between any two flashes of a storm.

The maximum interval predictand was chosen for several reasons. Fig. 5 displays the distribution of inter-flash times for the 116 storms comprising our dataset. The solid curve is the trend that is intuitively expected. That is, as a storm develops, the inter-flash times are large (i.e., the left side of the curve). The storm will have a peak of lightning activity in the mature stage (Byers and Braham 1949) that is evident with very small inter-flash times. Finally, as the storm reaches its dissipating stage, lightning activity diminishes, and the inter-flash times increase. If a storm experiences subsequent redevelopment or is multi-cellular in character, this trend might repeat itself. If lightning in all of our storms followed this cycle, the time between the last two flashes would be relatively easy to forecast.

However, as Fig. 5 shows, two additional lightning trends comprised a non-trivial portion of our dataset. Some storms had no true building phase during which the lightning activity slowly increased. Instead, the inter-flash times remain small from the storm's beginning and then exhibit the expected decay (dotted line). The third observed scenario (dashed line) shows a typical spin up, but then the storm suddenly stops producing lightning. This trend is troubling since the time between the last two flashes is small and would lead to an under-prediction of cessation wait times.

Based on the three scenarios in Fig. 5, it is apparent that the maximum interval can occur at any time during a storm's life cycle. Thus, the maximum interval initially does not appear to be a good choice for forecasting lightning cessation; however, additional factors had to be considered before making a final decision.

Figure 6 is a stylized example of several storms in our dataset. These storms initially produce a rapid series of lightning flashes (e.g., first five flashes) followed by a long delay. Then, several additional flashes occur in close succession at the end of the storm. This example exhibits two distinct time intervals. The interval between the last two flashes, i.e., between times 15 and 17, is 2 min. However, the maximum inter-flash interval occurs between 5 and 15 min, a delay of 10 min. We determined which interval to use in forecast development by examining both possibilities. We first assumed that the time between the last two flashes (2 min) should be used in our hypothetical forecast. We assumed that our forecast is perfect and that we could use 2 min as the time to wait after every flash (i.e., the time between the last two flashes) to decide if the flash just observed was, indeed the last one. This 2 min interval works well for the first four flashes since another flash always occurs within 2 min.

However, a problem occurs for the fifth flash. If the 2 min wait period is the only input, we would end our lightning advisory at 7 min, which would be an incorrect forecast since two additional flashes occur at 15 and 17 min, respectively. This means that equipment and personnel would be in danger since the lightning threat has not ended.

The alternate choice is to use the maximum interval between flashes, which in our hypothetical example is perfectly forecast to occur at 10 min. Using this interval, we correctly maintain the lightning advisory during the period between the 5th and 6th flashes. Additionally, our forecast waits long enough after the 7th (and last) flash to safely end the advisory.

The choice between using the time between the two last flashes or the maximum inter-flash time comes down to what is known versus what is not known in a real time setting. Unlike initiation, the forecaster's job for cessation is not finished with the first flash. Instead, the forecaster must decide if the flash that just occurred is the second to last flash; otherwise, he or she cannot use the forecast time between the previous two flashes because of the uncertainty of not knowing which flash has been observed. Thus, using the maximum predicted interval avoids this uncertainty by not forcing the forecaster to guess where in the sequence of flashes the observed flash occurs. If the forecast maximum inter-flash time interval has passed without another flash, the forecaster can confidently end the lightning advisory. The trade-off for using the maximum interval is the acceptance of over-forecasting the time to wait until the last flash.

With the characteristics calculated and the predictand chosen, we developed five schemes for providing cessation guidance. Four of the five schemes predicted the natural log of the maximum interval. The natural log was chosen since the raw maximum interval distribution was skewed to the right. The four schemes utilized multiple linear regression, correlation and regression tree analysis (CART), an event time trend (ETT), and a percentile method (PM). The sole exception was a scheme that attempted to predict the lag time between the time of the greatest height of the maximum dBZ of the storm (MZM) to the time of the last lightning activity.

All five schemes were derived using 100 storms randomly chosen from our dataset of 116 storms. The remaining 16 storms served as an independent verification dataset. Each scheme was tested against these remaining 16 storms and then compared against a 45WS forecast for the same 16 storms.

4. OBSERVED CHARACTERISTICS

Before presenting the prediction results, it is informative to describe some of the characteristics that were observed in our dataset. Several of these characteristics have not been discussed before or have been discussed only rarely.

4.1 Storm Characteristics

42 storms (36%) either are multi-cellular or exhibit some degree of redevelopment. Figure 7 is a histogram showing the duration of each storm, measured from the first flash to the last. The majority of storms (63%) last 40 min or less, with the longest lasting 138 min. 85 storms (73%) have 100 or fewer LDAR observed flashes, and of these, 50 contain twenty or fewer LDAR flashes. This relatively small number of large flash events results from the primary need for each storm to be fully isolated. Most large flash storms occurred in a cluster configuration which made isolating events very difficult. The most easily isolated storms were those having fewer flashes. The least active storm has 3 associated LDAR flashes, while the most active has 2,137.

4.2 LDAR Flash Characteristics

These characteristics were obtained using the flashes created from the raw LDAR data. Many of these characteristics cannot be used in real time, but do provide interesting insight into the storms.

The average inter-flash time of the LDAR-derived flashes (Fig. 8) is the time between the initiation of one flash to the initiation of the next flash. Average inter-flash times in our dataset range from a 3.4 s (0.6 min) minimum in a storm with 1711 LDAR-derived flashes to a maximum of 412 s (6.9 min) with three flashes. The median value for our 116 storms is 57 s. These values are influenced by the overall lightning activity of the individual storms since high activity storms generally reduce the average inter-flash rate.

The intra-cloud flash rate is another important variable describing our dataset. If this parameter were available in real time, it likely would be a powerful predictor of cessation. Our flash rates range from a minimum of 0.1 flashes min^{-1} to a maximum of nearly 18 flashes min^{-1}. The median is 1 flash min^{-1}. The distribution is skewed greatly to the right (not shown), with the majority of storms having fewer than 4 flashes min^{-1}. Current values are significantly smaller than those found by Wiens et al. (2005) who observed flash rates of nearly 300 flashes min^{-1}. However, it is important to note that Wiens et al. investigated a strong supercell over the Great Plains. Additionally, their 300 flashes min^{-1} included CG strikes, although IC

flashes comprised 95-100% of the total lightning activity. This may be misleading since their flash rate may have been increased by the flash creation algorithm being used, i.e. a single flash may have been broken into several flashes (Murphy 2006). Nonetheless, our small value may not be a representative sample of the total population of storms in the KSC area since our 116 storms were chosen to be fully isolated so we would know when the last flash occurred. Thus, results from many highly active storms had to be excluded from our dataset.

Individual flash characteristics are described next. The horizontal extent describes the distance (km) between the two most separated sparks in each flash of a storm (Fig. 9). The average horizontal extent of all flashes for all our storms is 12.8 km, ranging from a minimum of 3.9 km in a storm having 280 LDAR-derived flashes, to a maximum of 26.6 km in a storm with 122 flashes. McNamara (2002) studied the horizontal extent of only CG strikes in the KSC area, measuring the horizontal distance between the flash initiation point and the location of the CG strike. The horizontal extent of his CG strikes is expected to be smaller than our values since we observed the entire IC flash, which may extend well beyond the CG strike location. McNamara (2002) found that the average distance traveled by a CG strike was 8.7 km, with a maximum of 10.7 km and a minimum of 6.5 km. Nelson (2002) found that the mean horizontal distance from the LDAR initiation point to the most distant spark in the KSC area was 7.2 km, with 90% of the flashes having a horizontal extent of less than 16 km.

The average initiating altitude for our 116 storms is 7.4 km (Fig. 10), with a clear preference between 7 and 9 km. The minimum altitude is 4.5 km in a storm producing 6 flashes, and the maximum of 11.4 km occurs with a storm producing 506 flashes. An analysis of flashes using WDSS-II revealed that most flashes initiated in the storms' main updraft region, corresponding well to the findings of Carey et al. (2005).

4.3 LDAR Characteristics

Once it became clear that LDAR-derived flash characteristics could not be used in real time, the raw step leader data were used instead. These data were examined in case they contained similar descriptive information as the LDAR-derived flashes.

We first examined the total number of step leaders in a storm. This number is highly variable since it depends on a step leader's range from the LDAR network as well as the storm's overall activity. The storm with the smallest number had 41 step leaders that are consolidated into 4 flashes. Conversely, the storm with the greatest number has ~440,000 step leaders consolidated into 1426 flashes, which averages to 308 step leaders per flash.

The average altitude of all step leaders in a storm ranges from a minimum of 0.6 km in a storm producing 1426 flashes to a maximum of 10.2 km for 506 flashes. The average for all 116 storms is 7.8 km. This value is slightly higher than the 7.4 km average flash initiation altitude shown in Fig. 10. Figure 10 shows that the majority of flash initiation altitudes occur from 7 – 9 km, while the average step leader altitude (not shown) is slightly higher at 8 – 9 km. This compares well to the 8 – 11 km levels of maximum spark densities found by Carey et al. (2005) in a line of thunderstorms. The total number of step leaders at altitudes exceeding 10 km helps describes the intensity of a storm. The more intense storms, with correspondingly stronger updrafts, are expected to produce more lightning at altitudes exceeding 10 km. Four of our storms (3%) did not reach 10 km, and none of them had more than eight LDAR-derived flashes. An additional 32 storms (28%) had fewer than 50 step leaders above 10 km that were associated with no more than 51 flashes. Overall, the average value was ~7700 step leaders above 10 km, with the greatest being ~250,000 step leaders associated with 1426 flashes. The most electrically active storms (i.e., those with the most lightning) have the most step leaders above 10 km. Looking at the ratio of step leaders above 10 km to total step leaders appears to support this. Only 8 storms (7%) have more than ten thousand step leaders and have a ratio below 20%. Of these, only two have more than 15,000 step leaders. 82 (71%) storms have a ratio below 0.2. This is matches our distribution of total flashes with 85 storms with 200 or less flashes and only 9 of these 82 storms have more than 100 flashes. There are a few notable cases of storms with only high altitude lightning, but the number of step leaders above 10 km does appear related to total activity. Additionally, as the total flash count begins to exceed 300 flashes, the total number of step leaders above 10 km begins to number in the tens of thousands. This implies a stronger updraft that in turn implies the potential for a stronger charging and charge separation mechanism for the storm.

4.4 IC flashes versus CG strikes

The number of CG strikes versus IC flashes is discussed next. 96 storms (83%) have CG

activity, leaving 20 storms (17%) with only IC activity. This suggests that the previous studies using only cloud-to-ground lightning may have been good first approximations to the total lightning, though the best analysis is to use the actual total lighting, as we have done. The storms with only IC activity range from 3 flashes to 205 flashes. Conversely, two storms (1.7%) produce only CG strikes, yielding a CG strike percentage of 100%. These two storms each generate 6 strikes. The median percentage of total CG strikes in our storms is 14% although percentages reaching 50% are not uncommon. Only six storms (5%) have a percentage greater than 50%. Our median value is nearly three times greater than the 5% found by Wiens et al. (2005) for their single supercell.

It also is interesting to note whether the first and last lightning activity is IC or CG. In our 116 storms, 12 (10%) initiated with a CG strike, while 19 ended (16%) with a CG strike. Therefore, 104 storms (90%) initiated with an IC flash, while 97 storms (84%) ended in an IC flash. This agrees with Williams et al. (1989) and MacGorman et al. (1989) who indicated that IC activity typically precedes CG activity and with Weins et al. (2005) who found that IC activity greatly outnumbers the CG variety.

4.5 Environmental Characteristics

We compared our average initiation altitude with two sounding parameters that are related to lightning activity--freezing level height and wet-bulb zero pressure. Both parameters (not shown) show no trends when plotted against average initiation altitude. This was disappointing since both parameters indirectly relate to the presence of a mixed phase region within the cloud. The average initiation height above the freezing level is between 2-4 km. And, as expected, no storm has an average initiation altitude that is below the freezing layer height, and only a few individual flashes initiate below the freezing level. This most likely is a result of using the morning radiosonde data, which may not fully represent the environment at the time of the storm.

5. RESULTS AND VERIFICATION

All of the results that follow refer to Table 2 which shows the accuracy of each scheme, i.e., how often a lightning advisory is maintained long enough. Various over- and under-forecast errors also are presented. Additionally, two terms must be defined. The accuracy is the number of times the scheme waits as long as the maximum interval or longer divided by the total number of forecasts by the scheme. Accuracy was chosen to emphasize the importance of a forecast that does not under-predict lightning cessation. That is we reward a scheme that waits long enough for lightning to end, even if the wait is too long, i.e., an over-forecast.

The second term is precision. A precise forecast only slightly under- or over-predicts the maximum interval. It is possible for a scheme to be accurate, but not precise. This occurs when the scheme regularly forecasts the time of the maximum interval (accurate), but consistently over-forecasts the maximum interval (not precise). Since personnel safety is involved, the consequences of a premature cancellation of a lightning advisory are far more serious than maintaining the advisory too long. In other words, we prefer an over-forecast with virtually no chance of additional lightning instead of a more precise forecast with a greater chance of additional lightning.

5.1 The Percentile Method

The most successful scheme was the percentile method (PM). PM was derived from ten random samples of the 116 storms, where 12 different storms were omitted from each sample. Percentiles of maximum interval were calculated at the 50, 75, 95, and 99.5% levels from each sample (Fig. 11). Values of maximum interval at the 50th and 75th percentile levels were very similar among the ten samples. In contrast, the upper percentiles, particularly at 99.5%, were highly dependent on the specific greatest maximum interval storm(s) contained within the sample. The 95th percentile varied by 141 s (2.35 min) among the ten samples. At the 99.5% level, values ranged from 22.5 min when the greatest maximum interval storms were not included in the sample, to 25.5 min when all the largest maximum interval storms were included. This large variability at the highest percentile levels made it difficult to select any one of the ten as the defining sample. As a compromise, the results from all ten groups were averaged together. This yielded a time of 25.0 min at the 99.5% level.

When tested on our 16 independent storms, the PM is the most successful technique (Table 2). Although the detection rate is perfect at the 99.5% level, it comes with the trade off of large over-forecast times. Thus, the PM trades precision in wait time for accuracy (i.e., waiting at least as long as the actual maximum interval). PM's average error time is 18.1 min, while its median error is 21.2 min. These errors are the largest of any scheme by several minutes. PM's worst over-forecast time is 22.3 min. Although these errors

are large, one should note that it is the only technique that accurately forecasts all four large maximum interval storms within our 16 independent storm sample (Table 2). As a result of PM's perfect accuracy, there are no under-forecast storms and therefore no errors in under-forecast time. This is a very desirable characteristic.

PM is a true "rule of thumb" guideline. It requires no monitoring of parameters from radar or other sources. However, PM, like all of our schemes, needs observations of total lightning, including IC lightning, and therefore requires a total lightning observation network. PM is simple to use because each percentile risk level corresponds to an exact wait time since the previous flash. PM can be used any time of day and can be used in the morning to plan for afternoon activities. Additionally, the acceptance of risk by using lower percentiles can be included in these planning sessions.

Aside from the PM scheme, the remaining schemes had difficulty forecasting the maximum interval. The MZM method was our second best scheme in this regard.

5.2 Lag Time between the greatest altitude of maximum dBZ to the last lightning activity

The MZM method attempts to account for storm dynamics, namely the updraft, by utilizing radar data. It is an outgrowth of a technique suggested by Wolf (2006), where we attempted to reverse his lightning initiation criteria to forecast cessation. This research was limited since we did not have the same data as Wolf (2006), namely dBZ values at the -10°C level. In spite of the limitations, we hoped that using the lag time between the MZM and the last lightning would address the problem of forecasting the greatest maximum interval storms. In simplest terms, since the lag time is unrelated to the maximum interval, the scheme might be able to discern differences between the independent storms. MZM is plotted versus lag time in Fig. 12. A third order polynomial provides the best fit to the data, albeit poor, with an $R^2 = 0.349$.

The MZM trend is successful, particularly in terms of its excellent accuracy (88%). The large over-forecast errors (median 11.6 min) are accepted because of the scheme's high accuracy and small error in under-forecast times. The under-forecast error is respectable compared to the other schemes, with a median of 3.6 min. The scheme is easy to implement since only one predictor, the MZM, needs to be monitored in real time. Additionally, MZM is the only scheme that attempts to explicitly forecast the time to the last lightning activity. This creates opportunities for future research using improved radar data and testing new predictors such as the lag time to the last flash. Since MZM is the second best scheme, second only to PM, its ability to forecast when the last flash will occur could lead to a probability forecast that the last lightning activity has occurred once data better than available in our research can be utilized. MZM has the same operational constraint as the previous scheme (i.e., requires total lightning data), but MZM is not tracked until the first lightning activity in the storm is observed.

5.3 Storm Event Time Trends

Storm duration, the time between the first and last lightning activity, was selected as a predictor in many of our regression experiments (described later). This suggests that it may contain value when used alone. Similar to MZM, a cubic polynomial was fit to each storm's duration or event time (ETT) (not shown). The fit of the polynomial is poor ($R^2 = 0.079$) compared to that shown in Fig. 12 for MZM.

ETT is used by inputting the current storm event time into the cubic equation to get a forecast for the maximum interval. The forecast maximum interval gradually increases as the event time increases to ~60 min and then levels out.

The ETT proves reasonably successful. It is the third best overall scheme, with its important accuracy value being 81% (Table 2). ETT yields the best overall average and median forecast time errors of -0.1 and 1.6 min when the non-operational experimental regression (ER) scheme described next is not considered. Specifically, over-forecast timing errors are the best of any scheme with an average of 1.6 min and a median of 1.5 min. This is a surprising result since the schemes producing even better accuracies generally have greater over-forecast time errors, e.g., PM. However, ETT cannot match PM's confidence in knowing whether or not lightning activity has ceased. This is due to the weak relation between storm duration and the maximum interval. ETT is good at forecasting most of our independent storms, but the scheme fails for three of the four large maximum interval events.

5.4 Multiple Linear Regression

Three separate multiple linear regression approaches were tested, each based on forward stepwise regression. The most simple utilized only sounding parameters and is denoted the sounding only regression (SOR). The goal was to determine if the morning sounding could give a first guess

about afternoon lightning cessation. The second approach was the sounding and storm characteristic regression (SSR). It included the sounding predictors in SOR as well as real time predictors describing the storm itself (event time duration, spark height, and spark rate). Finally, an experimental regression (ER) was tested. Since so many LDAR-derived predictors could not be used in our schemes because they were not available in real time, the ER provides a "what if" scenario to determine what information these predictors would add if the raw LDAR data could be combined into flashes in real time.

When verified against the 16 independent storms, both the SOR and SSR equations produce poor results, achieving an accuracy of only 75%. Conversely, their average errors are two of the best at -0.17 and 0.2 min, respectively. The median over-forecast errors are 2.8 and 2.9 min, which are very good. However, the median under-forecast errors are 9.8 and 7.2 min, are the second and fourth worst, respectively. Furthermore, SOR and SSR produce very poor R^2 values of 0.08 and 0.295. This indicates that the schemes describe virtually none of the variability in the maximum interval and give no confidence in their forecasts, especially when compared to PM or MZM.

It is surprising that SSR yields the same accuracy and error statistics as SOR. This indicates that the inclusion of our real time storm parameters adds no additional information to the forecast. This suggests that the real time predictors that were available are not the best to describe the maximum interval. This is seen in the low correlations with the maximum interval (0.2 to 0.3). It is clear that better real time predictors, such as the radar parameters used by Wolf (2006) or LDAR-derived flash predictors should be investigated.

This latter conclusion is tested in the ER scheme. The primary predictor selected by ER was the average inter-flash rate for the storm. ER produced a dramatic drop in the error of the forecasts that coincided with a dramatic drop in forecast accuracy. The accuracy dropped to 44%; the worst of any scheme. However, the scheme yields the best forecast errors in all categories except for average over-forecast time (Table 2). Specifically, the overall average and median forecast errors are 0.1 and -0.1 min, respectively. The average and median under-forecast errors are 2.7 and 0.8 min, compared to values between 6 and 9 min for SOR and SSR schemes (Table 2). ER's under-forecast errors are half to a third of those for the other schemes. The average and median over-forecast time errors are 3.7 and 1.0 min, respectively.

The error statistics indicate that ER has more precision than the other schemes. The trade off for this improved precision is ER's very low accuracy. Unlike some schemes that achieve high accuracy with large over-forecast errors, ER attempts to predict the exact maximum interval (i.e., with very little forecast error). The R^2 value jumps to 0.54, which is a major improvement over SOR and SSR, but is still below what is desirable (e.g., 0.8-0.9).

ER's single greatest over-forecast error deserves discussion. This value of 19.4 min is the third worst of our schemes. However, it occurred when trying to forecast a storm with a maximum interval of 22 min, which most of our schemes had great difficulty with. In fact, ER is one of only two other schemes that successfully forecast even one of the 4 storms with a large maximum interval. It obviously is very important to successfully forecast these outlier storms, and ER is one of the only schemes to show the potential to do so. Therefore, the ER approach requires further study if a method can be devised to consolidate LDAR sparks into flashes in real time.

Even with its poor accuracy, ER has potential as demonstrated by its precision. If real time LDAR-derived flash parameters and better radar-derived parameters become available, ER might reasonably forecast the maximum interval times. This could lead to decreased over- and under-forecast errors and to increased accuracy. Thus, ER could have value when used in concert with PM. PM would provide a general forecast, while ER would provide details about each specific storm.

5.5 Correlation and Regression Tree Analysis

Our worst scheme was correlation and regression tree analysis (CART, Brieman et al. 1984; Venables and Ripley 1997; Burrows 2004) whose approach is similar to SOR and SSR. The final CART algorithm selected several types of predictors, the time between the first IC flashes and first CG strikes plus storm duration (i.e., storm specific information), and vertical wind shear through 6 km plus the bulk lifted index (BLI) (i.e., the type of thunderstorm and intensity that are expected).

The final decision tree (Fig. 13) contains six decision points with seven termination nodes. Times at the termination nodes are important descriptors to discuss. The greatest termination value is 10.9 min, considerably less than the maximum interval of three of our 16 independent

storms, which are as long as 22 min. This automatically creates three under-forecast events, which reduces CART's best accuracy to 81% if every other forecast is correct.

Three of the first four nodes (Fig. 13) are based on the time delay between the first IC flash and the first CG strike. This parameter ranges from 0.8 to 13.4 min for our independent storms, with three events having no CG activity. If there was no associated CG, the lag was assumed to be infinite, and events with coincident IC and CG had a lag time of 0 min. Lag time was useful to discriminate between the small and moderate maximum interval storms that comprised 12 of the independent cases. However, CART predicted none of the four greatest maximum interval storms to have a 10.9 min time because the lag times between the first IC and CG strike were either too small, or the shear was too large. Because of these parameters, CART's forecast is shifted to the right side of the decision tree where the predicted maximum intervals range from 3 to 8 min, all of which are under-predictions of the maximum intervals for the four greatest maximum interval storms.

CART produces an accuracy of 56% (Table 2) which is the second worst of any scheme and the worst when not considering the non-operational ER. Under-forecast times are another major limitation, with a median under-forecast time of 3.2 min, including one event that is under-predicted by ~20 min. Although the median under-forecast value is good compared to most other schemes, its large average indicates a wide range of under-forecasting the maximum interval. Overall, the average timing error is -1.5 min, with a median of 0.3 min, and no event is over-forecast by more than 6 min. Although the over-forecast is good, it is worthless due to the poor accuracy.

Since our storms were historical events, we had information up to their demise. However, in an operational setting, forecasters would have to update the input to the algorithm as the storm evolved. We had hoped that this ability to adjust the cessation forecast during a storm's life cycle would be an important positive attribute of the CART procedure. However, even if this adjustment could be performed in real time, the disappointing results are not worth the effort.

5.6 Comparison to 45WS Advisories and the 30/30 Rule

The 45WS does not have one specific time interval to wait after a particular flash before canceling a lightning advisory (Personal communications Boyd 2007; McNamara 2007; Roeder 2007). This arises from the uncertainty of lightning cessation associated with different environmental conditions. Although the 45WS believes that their advisories are maintained too long, there are no formal statistics. The 45WS uses two "rules of thumb". Based on Air Force guidelines, they wait between 15-20 min after each flash before ending an advisory. However, if stability conditions favor storm redevelopment, this time can be extended to 30 min. A final extension can occur if the criteria for anvil or debris lightning initiation have not ended. Anecdotally, 45WS forecasters may exceed these guidelines in real-world practice, in the absence of objectively quatittively verified techniques and in the interest of personnel safety.

30 min also is the wait time of the 30/30 rule. This simple lightning safety rule states that an individual should be in a safe place by the time the whe the delay beteen thunder and its lightning is 30 s or less, and should remain in shelter for 30 min after the last thunder.

This section focuses on over-forecasts and their associated time savings compared to those of the three 45WS wait times just described. Table 3 contains median over-forecast errors and accuracies for the three 45WS wait times when applied to our 16 independent storms. If any of our schemes improves the wait times compared to the current 45WS standards, there will be an economic benefit.

Table 4 shows the time savings or penalty of our schemes when compared to median over-forecast errors based on the 45WS wait times (15, 20, and 30 min, Table 3). Time savings is indicated by a negative value (i.e., our scheme waits less than the 45WS), while a penalty is indicated by a positive value (i.e., our scheme waits longer than the 45WS). The results show that time savings is inversely proportional to accuracy. For example, our scheme with the best accuracy (100%), the 99.5% confidence level from PM, has the greatest median over-forecast error (21.2 min). It only produces a time savings when the 45WS waits 30 min. Conversely, the ER scheme has the worst accuracy (44%), yet the smallest median over-forecast error.

Although PM provides relatively small time savings, its important strength is forecast confidence. When compared to the 45WS's most conservative wait time of 30 min and the 30/30 rule, the PM scheme at the 99.5% confidence level provides a 5 min time savings. This is a good result, saving time compared to the 45WS and with the near certainty that further lightning will not occur.

MZM and PM at a 95% confidence level are our only other schemes that equal the 45WS wait time accuracy of 88% (Table 2 and 3). The 95% confidence level is equal to the shortest 45WS wait time, 15 min. Therefore, the 95% confidence level quantifies the risk of waiting 15 min. The risk is 5% that additional lightning will occur after the scheme forecasts the all clear. MZM has the same accuracy as the 15 and 20 min 45WS wait times. However, MZM produces an excellent time savings of 4.6 and 14.6 min over the 20 and 30 min 45WS wait times. This comes with a 12% risk of future lightning.

Every other scheme produces a time savings that is much better than the three 45WS wait times, sometimes ending advisories 20 min earlier. However, the accuracy of these schemes is worse than those of the 45WS. As a result, they provide no certainty and thus are less safe than current procedures. As stated earlier, schemes with the worst accuracy generate the best time savings. This means that when the poor accuracy schemes are correct, they provide great benefit to ending lightning advisories. Unfortunately, their accuracy is too low to safely end the advisories.

Safety is the primary concern when deciding when to end a lightning advisory. Therefore, we prefer a procedure with high accuracy but diminished time savings (i.e., precision) over a scheme that gives excellent time savings but leaves too much uncertainty as to whether lightning activity actually has ended. Therefore, our three most recommended schemes are the MZM lag and the 95% and 99.5% levels of PM. PM's 99.5% confidence level is the most recommended since it is the only procedure that successfully forecasts all four of the large maximum interval storms within our 16 independent storms. PM also provides near certainty that lightning has ceased if high percentiles are selected.

Additional statistics were calculated, but accuracy is the main measure of success as it accounts for a schemes ability to maintain a lightning advisory long enough for cessation to occur. The mean square error (MSE) was calculated for each scheme (not shown) that resulted in several of the low accuracy schemes to have low MSEs compared to the PM scheme. This is not surprising as several of the low accuracy schemes have low under- and over-forecast errors, particularly ER. As a result, their forecasts are close to the observed maximum interval time, reducing the MSE. However, a good MSE does not mean a good accuracy, as these schemes end advisories too early.

A ratio skill score (RSS) was computed for each scheme. This is simply a briar skill score that uses the 45WS forecasts as the climatology. The issue is that the 30 minute wait time of the 45WS is "perfect" and remains in effect long enough for lightning activity to cease. As a result, only the PM at 99.5% matches the 45WS at 30 min and every other scheme has no true solution as our reference state is perfect and we divide by zero. Even with the shorter and less accurate 45WS times of 15 and 20 minutes, the RSS for the majority of the schemes are negative, indicating no skill improvement, as supported by their poor accuracy scores.

This means that our accuracy score and the over-forecast errors give the most meaningful results. Higher accuracy is the most desirable result followed by a time savings versus the 45WS scores. In this, the PM at 99.5 and 95% as well as the MZM are the most recommended schemes.

6. SUGGESTED FUTURE RESEARCH

Several avenues for future research are available. The easiest method is to expand the sample size of the dataset to include more storms. Additionally, efforts to incorporate more complex storms as well as storm types are encouraged, although determining which storm a flash originates from remains challenging. Additionally, this research has utilized data from the warm season months of May through September. These same schemes can be tested on non-warm season storms.

Future research also should focus on obtaining the LDAR-derived flash parameters in real time since some type of ER scheme may be able to forecast the maximum interval better than any of our current techniques. In essence, ER may be a more "dynamical" scheme that can forecast the actual predictand. A more synergistic approach using both PM and an improved ER scheme could provide an excellent future forecast guidance. PM would provide a "climatology" of maximum intervals for early planning, while ER could give more precise forecasts that are accurate and thereby reduce over-forecast errors. This research has emphasized accuracy above all else. The goal of this future research will be to expand on the PM's accuracy while at the same time increasing precision. This would result in lower MSE scores and improved RSS scores.

Additional work with WDSS-II is currently underway at Florida State. Here, flash densities are being created from the existing LDAR dataset. This is being combined with flash rates, flash altitudes, and other parameters for relation with

radar and CG data. The overall goal is to analyze a multitude of storms instead of single storms only.

Lastly, improved radar data compared to this research is recommended. This has two approaches. First, a more concerted effort to reverse the Wolf (2006) scheme is recommended. Wolf (2006) used combinations of radar values and temperature levels. This extra level of detail can be applied as possible predictors in our scheme. Secondly we believe that microphysical parameters will be necessary to further improve on our schemes and to create a technique that more precisely forecasts lightning. Dual poloarization radar can be used to detect mixed phase hydrometeors, which may lead to a decay time based on ice mass for Z-M relationships. Dual polarization radar also may lead to a direct calculation.

7. SUMMARY

Our main objective was to expand on the studies (Hinson 1997; Holmes 2000; Roeder and Glover 2005) by including LDAR data from KSC. Data from CGLSS, morning radiosonde launches, and the WSR-88D, assembled 100 potential cessation characteristics. This was reduced to 33 candidate predictors (Table 1).

The time between the last two flashes seemed to be the intuitive choice, but the maximum interval between any two flashes ultimately had the smallest number of complicating issues. Five schemes were created from randomly selecting 100 of our 116 storms. The schemes were verified against the remaining 16 storms and the average wait times of the 45WS (Tables 3, 4).

Accuracy was the primary verification statistic rewarding schemes that waited long enough for lightning to end, which accepted over-forecast errors. Safety drove this, as we wanted a scheme that predicted with great certainty that lightning had ended, instead of a scheme that merely produced small errors. The best accuracies were achieved with the PM, MZM lag, and ETT techniques. Overall, the most successful scheme was PM at 99.5%, saving 5 minutes over the most conservative 45WS times.

LDAR-derived flash parameters were not allowed in our schemes as much as had been anticipated, except in the ER procedure. Their omission wass because LDAR step leaders cannot be consolidated into flashes in real time. When the LDAR-derived flash parameters were allowed in ER, poor accuracy was obtained; however, their inclusion did produce the best timing errors. These small errors indicated that ER forecasts were closer to the actual values of maximum interval than any other scheme. Future work should focus on obtaining the real time LDAR parameters and combining the results with the PM scheme and improved radar data.

The reader should be aware that our findings are based on warm season (May-September) isolated storms.

8. ACKNOWLEDGEMENTS

Special thanks go to Todd McNamara of the 45th Weather Squadron for his help with several technical aspects of this research and to the numerous individuals who provided their critiques at the *1st International Lightning Meteorology Conference (ILMC)* in Tucson, AZ in 2006.

This research was sponsored by NASA's Innovative Partner's Proposal Program under Grant NNK06EB17G.

9. REFERENCES

Boccippio, D. J., S. J. Heckman, and S. J. Goodman, 2001: A diagnostic analysis of the Kennedy Space Center LDAR network. 1. Data characteristics. *J. Geophys. Res.*, **106**, 4769-4786.

Bott, T. F., and S. W. Eisenhawer: Development of optimal lightning warning procedures using probabilistic risk analysis.

Boyd, B. F., W. P. Roeder, J. B. Lorens, D. S. Hazen, and J. W. Weems, 1995: Weather support to pre-launch operations at the Eastern Range and Kennedy Space Center. Preprints, *Sixth Conf. on Aviation Weather Systems*, Dallas, TX, Amer. Meteor. Soc., 135-140.

Boyd, B. F., W. P. Roeder, D. L. Hajek, and M. B. Wilson, 2005: Installation, upgrade, and use of a short baseline cloud-to-ground lightning surveillance system in support of space launch operations, *Conference on Meteorological Applications of Lightning Data*, 9-13 Jan 05, 4 pp.

Boyd, B. F., 2007: Personal communication. 45th Weather Squadron, Cape Canaveral, Florida.

Brenner, I. S., 2004: The relationship between meteorological parameters and daily summer rainfall amount and coverage in West-Central Florida. *Wea. Forecasting*, **19**, 286-300.

Brieman, L., Friedman, J. H., Olshen, R. A., and C. J. Stone, 1984: *Classification and Regression Trees*. CRC Press, 358 pp.

Britt, T. O., C. L. Lennon, and L. M. Maier, 1998: *Lightning Detection and Ranging System*. NASA Tech Brief, Vol. 22, Issue 4, 60-61.

Burrows, W. R., Price, C., and Wilson, L. J., 2004:

Statistical models for 1-2 day warm season lightning prediction for Canada and the Northern United States. Preprints, *17th Conference on Probability and Statistics in the Atmospheric Sciences*, Seattle, WA, Amer. Meteor. Soc.

Byers, H. R., and R. R. Braham, 1949: *The Thunderstorm*. Supt. Of Documents, U.S. Government Printing Office, Washington D.C., 287 pp.

Carey, L. D., M. J. Murphy, T. L. McCormick, N. W. S. Demetriades, 2005: Lighting location relative to storm structure in a leading-line, trailing-stratiform mesoscale convective system. *J. Geophys. Res.*, **110**.

Cummins, K. L., M. J. Murphy, E. A. Bardo, W. L. Hiscox, R. B. Pyle, and A. E. Pifer, 1998: A combined TOA/MDF technology upgrade of the U.S. National Lightning Detection Network, *Journal of Geophysical Research*, **103**, 9035-9044.

Cummins, K. L., R. B. Pyle, and G. Fournier, 1999: An integrated American lightning detection network, *11th International Conference on Atmospheric Electricity*, 7-11 Jun 99, 218-221.

Curran, E. B., R. L. Holle, and R. E. Lopez, 2000: Lightning fatalities, injuries and damage reports in the United States, 1959-1994, *J. Clim.*, **13**, 3448-3453.

Hinson, M. S., 1997: A study of the characteristics of thunderstorm cessation at the NASA Kennedy Space Center, *M.S. Thesis*, Aug 97, Texas A&M University, 91 pp.

Hodanish, S., D. Sharp, W. Collins, C. Paxton, R. E. Orville, 1997: A 10-yr monthly lightning climatology of Florida: 1986-95. *Wea. For.*, **12**, 439-448.

Holmes, M. W., 2000: Techniques for forecasting the cessation of lightning at Cape Canaveral Air Station and the Kennedy Space Center, *M.S. Thesis*, Air Force Institute of Technology, 90 pp.

Holle, R. L., López L. J., R. Ortiz, A. I. Watson, D. L. Smith, D. M. Decker, and C. H. Paxton, 1992: Cloud-to-ground lightning related to deaths, injuries, and property damage in Central Florida. Proceedings, International Aerospace and Ground Conference on Lightning and Static Electricity, Atlantic City, New Jersey, FAA Report No. DOT/FAA/CT-92/20, 66-1-66-11.

Lakshmanan, V., T. Smith, G. J. Stumpf, and K. Hondl, 2007: The warning decision support system - integrated information (WDSS-II). *Weather and Forecasting*, **22**, No. 3, 592-608.

Lennon, C. L., 1975: LDAR—A new lightning detection and ranging system. *Eos, Trans. Amer. Geophys. Union,* **56,** 991.

Livingston, E. S., J. W. Nielson-Gammon, and R. E. Orville, 1996: A climatology, synoptic assessment, and thermodynamic evaluation for cloud-to-ground lightning in Georgia: A Study for the 1996 Summer Olympics. *Bull. Amer. Meteor. Soc.*, **77**, 1483-1495.

Lopez, R. E., P. T. Gannon, Sr., D. O. Blanchard, and C. C. Balch, 1984: Synoptic and regional circulation parameters associated with the degree of convective shower activity in South Florida. *Mon. Wea. Rev.*, **112**, 686-703.

MacGorman, D. R., D. W. Burgess, V. Mazur, W. D. Rust, W. L. Taylor, and B. C. Johnson, 1989: Lightning rates relative to tornadic storm evolution on 22 May 1981. *J. Atmos. Sci.*, **46**, 221-250.

Maier, L. M., C. Lennon, T. Britt, and S. Schaefer, 1995a: Lightning Detection and Ranging (LDAR) system performance analysis. Preprints, *Sixth Conf. on Aviation Weather Systems*, Dallas, TX, Amer. Meteor. Soc., 305-309.

McNamara, T. M., 2002: The horizontal extent of cloud-to-ground lightning over the Kennedy Space Center, *M.S. Thesis*, Air Force Institute of Technology, 114 pp.

McNamara, T. M., 2007: Personal communication. 45th Weather Squadron, Cape Canaveral, Florida.

Murphy, M. J., K. L. Cummins, and L. M. Maier, 2000: The analysis and interpretation of three-dimensional lightning flash information. *16th Int. Conf. on IIPS for Meteorology, Oceanography, and Hydrology*, Long Beach, CA, Amer. Meteorl. Soc., 102-105.

Murphy, M. J., 2006: When flash algorithms go bad. *1st International Lightning Meteorology Conference*, Tucson, AZ, 26-27 Apr 06, 6 pp.

Nelson, L. A., 2002: Synthesis of 3-dimensional lightning data and radar to determine the distance that naturally occurring lightning travels from thunderstorms, *M.S. Thesis*, Air Force Institute of Technology, 85 pp.

Neumann, C. J., and J. R. Nicholson, 1972: Multivariate regression techniques applied to thunderstorm forecasting at the Kennedy Space Center. Preprints, *International Conference on Aerospace and Aeronautical Meteorology*, Washington D.C., Amer. Meteor. Soc., 6-13.

Orville, R. E., 1994: Cloud-to-ground lightning flash

characteristics in the contiguous United States: 1989-1991. *J. Geophys. Res.*, **99,** 10 833-10 841.

Orville, R. E., and G. R. Huffines, 2001: Cloud-to-ground lightning in the United States: NLDN results in the first decade, 1989-98. *Mon. Wea. Rev.*, **129,** 1179-1193.

Orville, R. E., G. R. Huffines, W. R. Burrows, R. L. Holle, and K. L. Cummins, 2002: The North American Lightning Detection Network (NALDN) –first results: 1998-2002. *Mon. Wea. Rev.*, **130,** 2098-2109.

Poehler, H. A., and C. L. Lennon, 1979: *Lightning Detection and Ranging (LDAR) System Description & Performance Objectives*. NASA Technical Memorandum 74106, 86 pp.

Roeder, W. P., J. T. Madura, and D. E. Harms, 2000: Lightning safety for personnel at Cape Canaveral Air Force Station and Kennedy Space Center, *Joint Army Navy NASA Air Force / Safety & Environmental Protection Symposium*, 8-12 May 00, Cocoa Beach, FL, CPIA Pub 698, 59-70.

Roeder, W. P., and J. E. Glover, 2005: Preliminary results from phase-1 of the statistical forecasting of lightning cessation project, *Conference on Meteorological Applications of Lightning Data*, 9-13 Jan 05, 6 pp.

Roeder, W. P., J. W. Weems, and P. B. Wahner, 2005: Applications of the Cloud-to-Ground Lightning Surveillance System database. *Conf. on Meteorological Applications of Lightning Data*, 9-13 Jan 05, 5 pp.

Roeder, W. P., 2007: Personal communication. 45th Weather Squadron, Cape Canaveral, Florida.

Shafer, P. E., and H. E. Fuelberg, 2006: A statistical procedure to forecast warm season lightning over portions of the Florida peninsula. *Wea. Forecasting*, **21**, 851-868.

Venables, W. N., and B. D. Ripley, 1997: *Modern Applied Statistics with S-Plus*. Springer-Verlag, New York, 548 pp.

Weems, J. W., C. S. Pinder, W. P. Roeder, and B. F. Boyd, 2001: Lightning watch and warning support to spacelift operations, *18th Conference on Weather Analysis and Forecasting*, 30 Jul-2 Aug 01, 301-305.

Wiens, K. C., S. A. Tessendorf, and S. A. Rutledge, 2005: June 29, 2000 supercell observed during STEPS. Part II: Lightning and charge structure. *J. Atmo. Sci.*, **62**, 4151-4177.

Williams, E. R., M. E. Weber, and R. E. Orville, 1989: The relationship between lightning type and convective state of thunderclouds. *J. Geophys. Res.*, **94**, 13213-13220.

Wolf, P., 2006: Anticipating the initiation, cessation, and frequency of cloud-to-ground lightning, utilizing WSR-88D reflectivity data. NOAA/National Weather Service, Jacksonville, Florida.

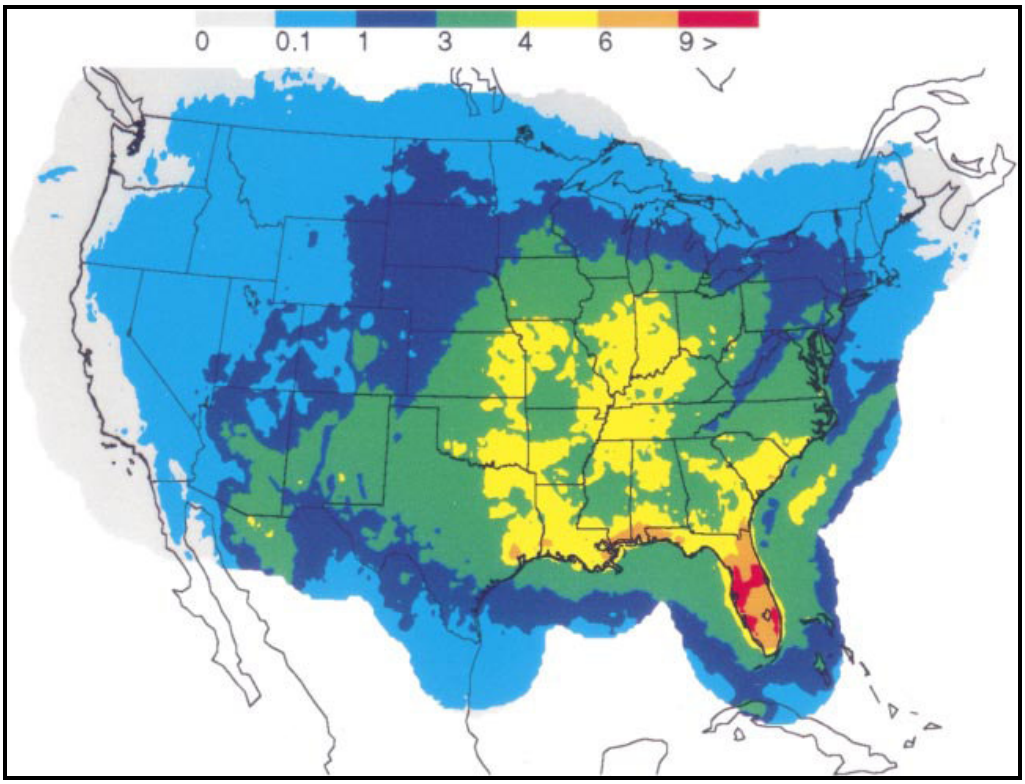

Figure 1. Mean annual CG flash densities (flashes km^{-1} $year^{-1}$) from 1989 to 1998. Note the maximum greater than 9 flashes km^{-1} $year^{-1}$ over Central Florida. (After Orville 1994).

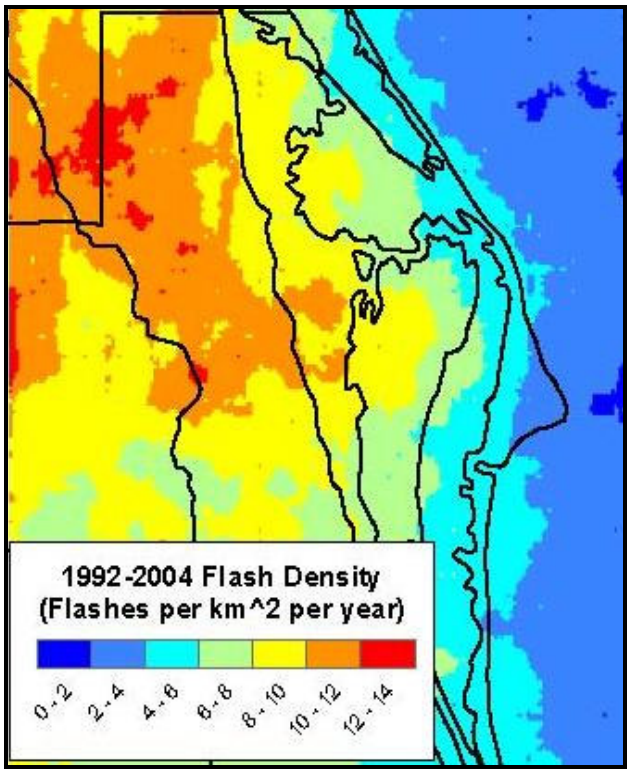

Figure 2. Annual CG flash densities over east Central Florida (flashes km^{-1} $year^{-1}$) from 1992 to 2004. Note that the KSC region receives between 4-10 flashes km^{-1} $year^{-1}$.

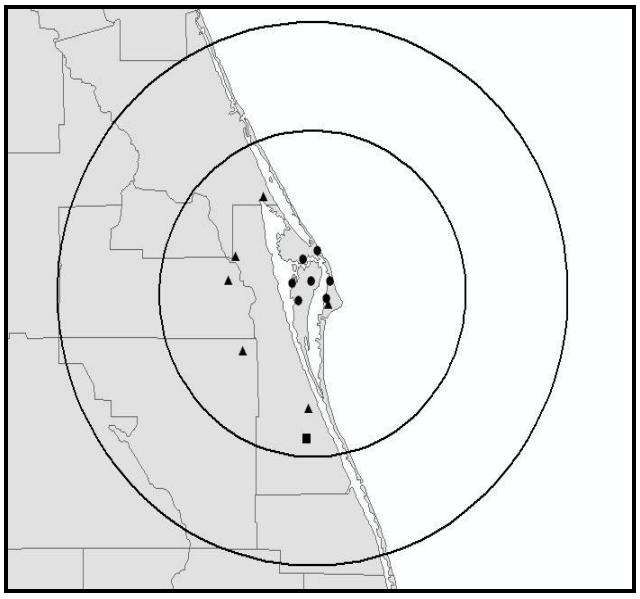

Figure 3. Domain of the research, where the outer ring is 100 km from the center of the LDAR network and the inner ring is at 60 km. Priority was given to events occurring within 60 km, and no event was further than 100 km. The location of the main observation networks are shown for LDAR (circles), CGLSS (triangles), and the WSR-88D (square).

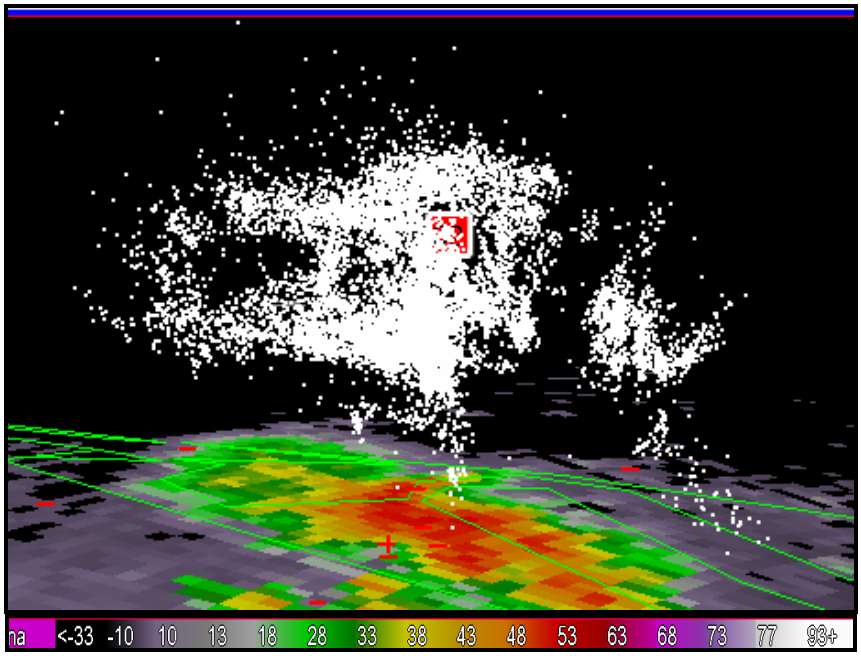

Figure 4. Sample image from the WDSS-II software over the Kennedy Space Center. The view is from the southwest overlooking Cape Canaveral at an elevation angle of ~50°. Colors at the surface are a plane view of radar reflectivity, while the '+' and '-' signs represent CG strike locations. White dots are the individual stepped leaders (e.g., sparks) of multiple intra-cloud flashes observed by the LDAR network. CG strikes are associated with downward propagating sparks. The dBZ scale is given below the image.

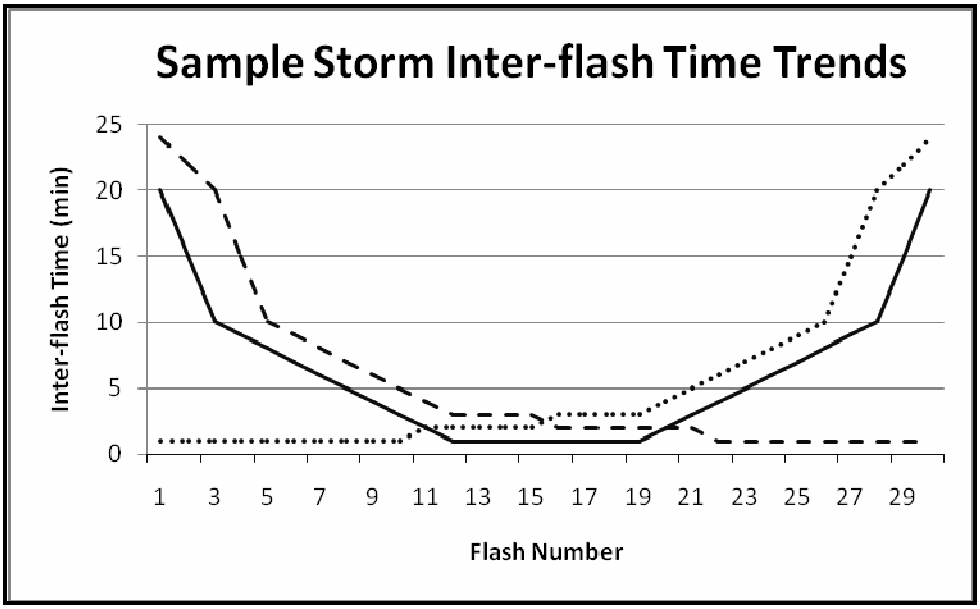

Figure 5. Illustration of the three common distributions of a storm's inter-flash time. The majority of our storms had the u-shaped distribution (solid line); however, other storms had either a rapid initiation and slow decay (dotted), or slow initiation and rapid decay (dashed), that made it difficult to use the time between the last two flashes as a predictand.

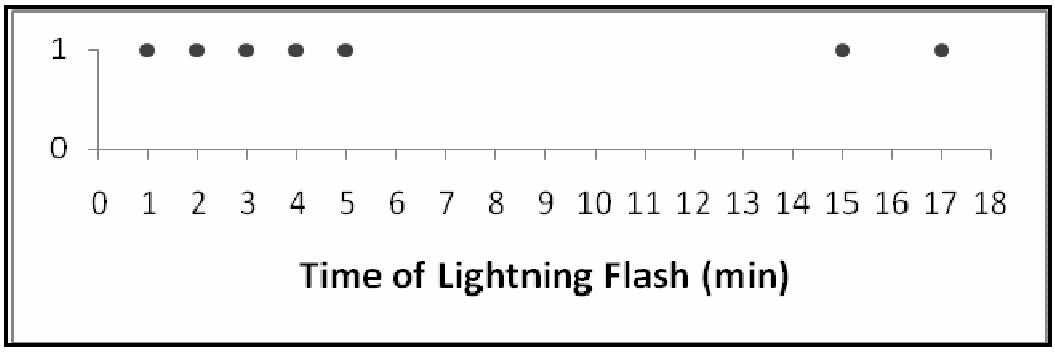

Figure 6. Illustration supporting the use of the maximum time interval between flashes instead of the time between the last two flashes. In 68% of the events, the maximum interval was greater than between the last two flashes, making the former the superior variable to forecast lightning cessation.

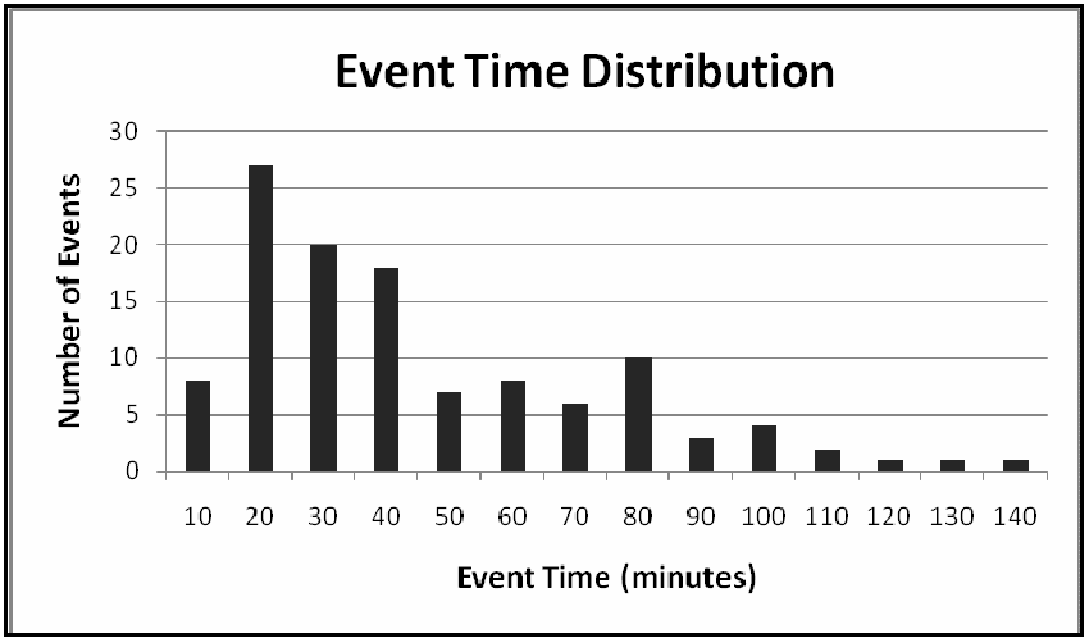

Figure 7. The distribution of isolated thunderstorms with respect to their total duration in minutes (from the first LDAR observed flash to the last).

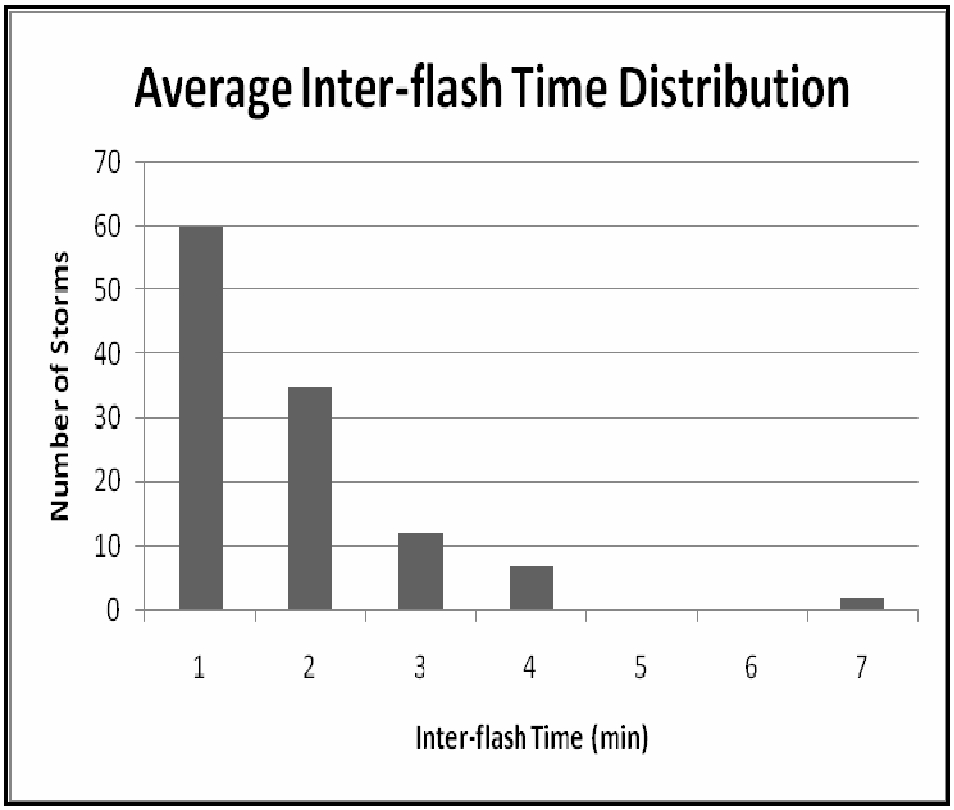

Figure 8. Distribution of the average inter-flash time (min) for our 116 storms.

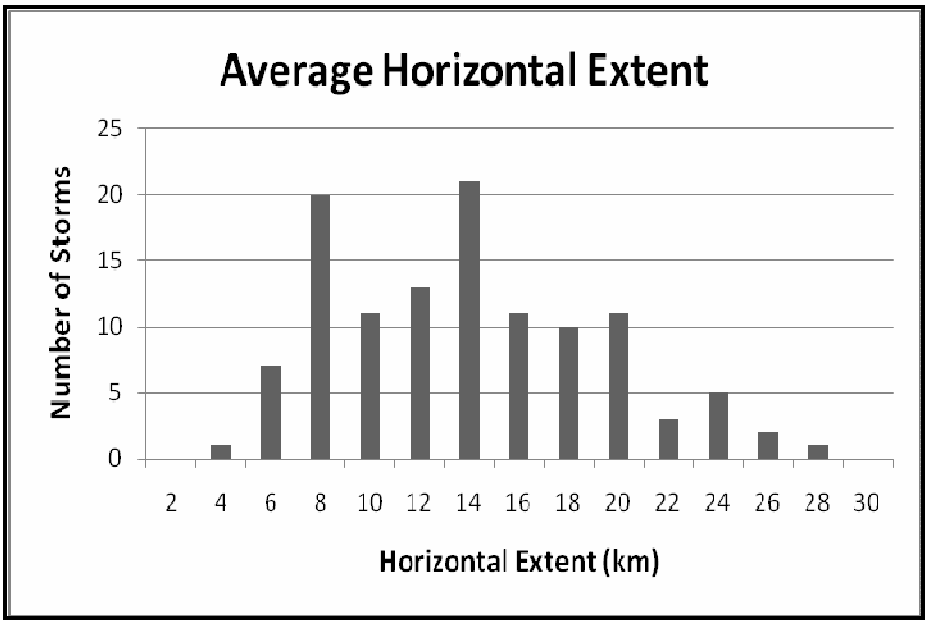

Figure 9. Distribution of the average horizontal extent (km) from the two most distant sparks in a flash for our 116 storms.

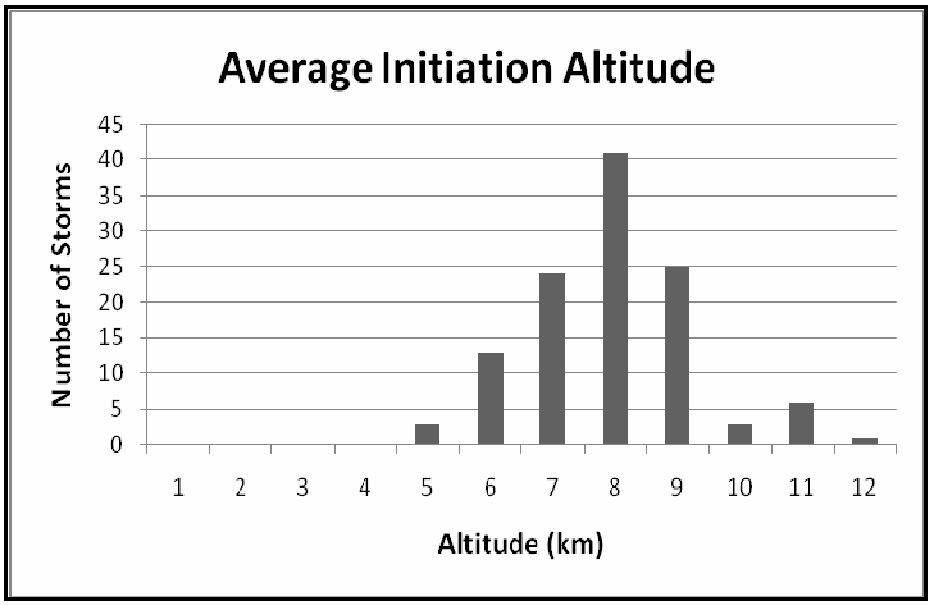

Figure 10. Distribution of the average initiation altitude (km) for each flash in our 116 storms.

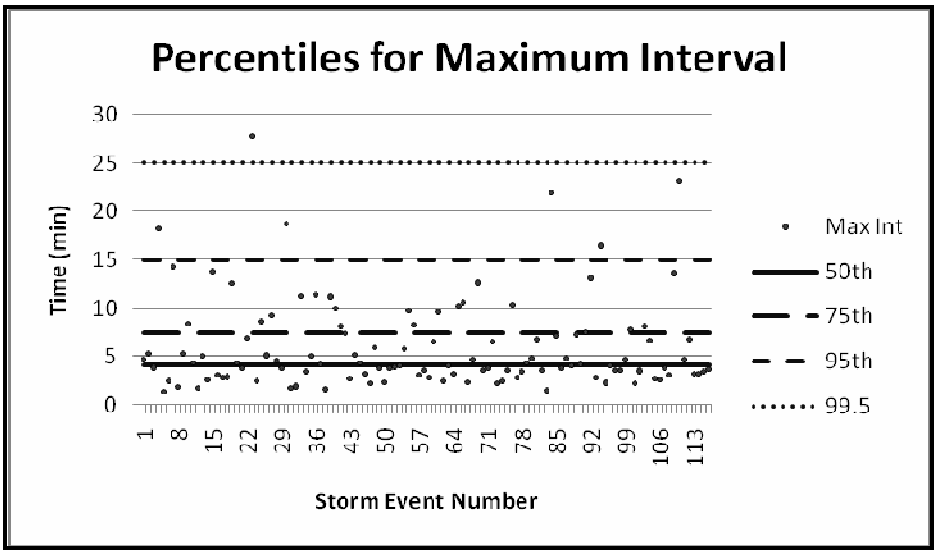

Figure 11. Maximum interval times (min) for each thunderstorm event in our data set. The corresponding 50th (4.17 min – solid), 75th (7.5 min – long dash), 95th (15 min – short dash), and 99.5th (25 min – dotted) percentiles are superimposed.

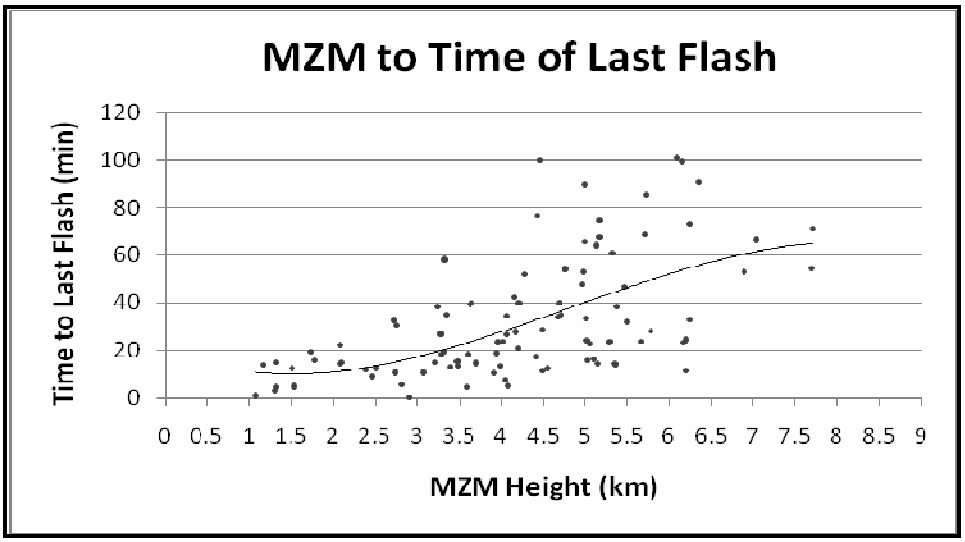

Figure 12. Scatterplot of the maximum height of the maximum dBZ (MZM) in km versus the time to the last flash (min).

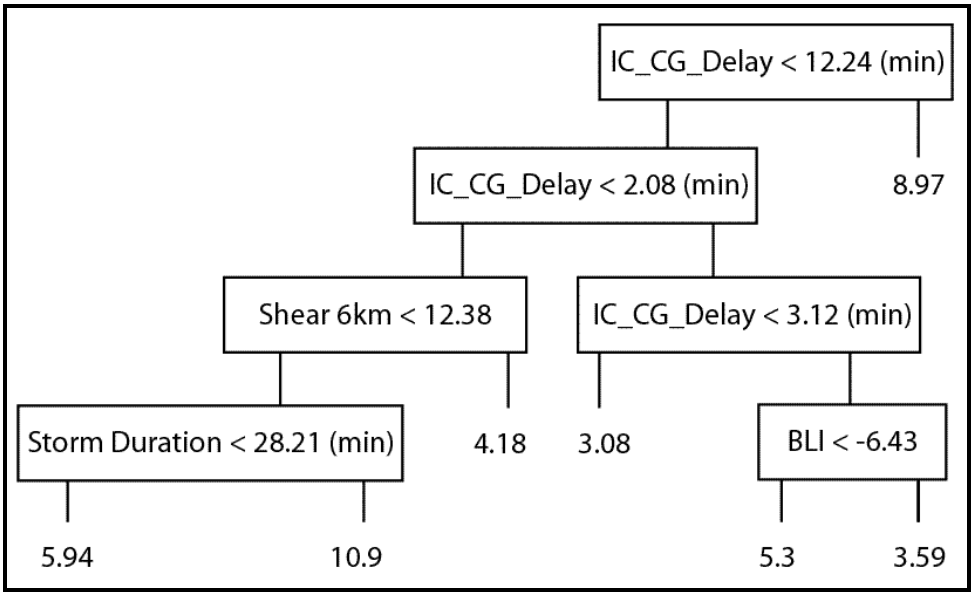

Figure 13. Flowchart for the best CART analysis. Numbers at the end nodes are the maximum interval times in minutes.

Table 1. The final 33 candidate parameters that were used in the various guidance schemes created for this research. Each parameter had a co-linearity of less than 0.6 with every other parameter. (C: CGLSS, L: LDAR, R: Radar, S: Sounding)

Time from maximum VIL to final flash (min) – R	Average inter-flash time interval (s) – L	Time between the last two flashes – L	Storm duration from the first to last flash (min) – L	Average flash horizontal extent (km) – L
Convective temperature (K) – S	Convective Condensation Level (CCL) (hPa) – S	Mean relative humidity through 1 km (%) – S	Average time between the last 5 flashes (s) - S	Total sparks for thunderstorm – L
Theta-E lapse rate between 950 – 700 (hPa) – S	Maximum VIL of the thunderstorm – R	Total CG of the thunderstorm - C	Mean wind direction (1000 – 700 hPa) (deg) - S	Average flash starting height (km) – L
Shear through 6 km – S	Shear through 500 – 200 hPa - S	Wet bulb zero level (hPa) – S	Best lifted index (°C) – S	Delay between first IC and first CG (min) – L and C
Storm over land or water – L	Whether first flash was IC or CG – L and C	CG strike rate (per min) - C	Precipitable water (in) – S	-40°C level (hPa) – S
Showalter index – S	Freezing level (m) – S	Convective inhibition (CIN) (J kg^{-1}) – S	Percentage of CG to IC – L and C	Maximum height of maximum dBZ for the thunder-storm (m) – R
Most unstable CAPE (MUCAPE) (J kg^{-1}) – S	Number of sparks above 10 km – L	Average spark height (km) - L		

Table 2. Summary table of basic results from the five empirical schemes. Three schemes were based on regression models (SOR, SSR, and ER). Note that the MZM lag predicts the time to the last flash and not the maximum interval between flashes.

Scheme	**CART**	**SOR**	**SSR**	**ER**	**ETT**	**MZM LAG**	**99.5% LEVEL**	**95% LEVEL**
R^2	--	0.08	0.295	0.54	--	--	--	--
Accuracy (%)	56	75	75	44	81	88	100	88
Average Error (min)	-1.5	-0.17	0.2	0.1	-0.1	13.5	18.1	8.1
Median Error (min)	0.3	2.3	2.4	-0.1	1.6	9.2	21.2	11.2
Greatest Under	19.6	15.9	11.5	13.4	12.9	6.5	--	8.2
Average Under	6.2	9.1	6.9	2.7	10.1	3.6	--	7.6
Median Under	3.2	9.8	7.2	0.8	10.6	3.6	--	7.6
Greatest Over	5.2	4.5	4.4	19.4	5.4	43.8	22.3	12.3
Average Over	2.2	2.8	2.7	3.7	1.6	15.9	18.1	10.4
Median Over	1.8	2.9	2.8	1.0	1.5	11.6	21.2	11.2

Table 3. Median over-forecast times for the three 45WS wait periods of 15, 20, and 30 min. The accuracy for each wait time also is provided for our dataset.

45WS Wait Time	Median Over-Forecast Error (min)	Accuracy (45WS Wait Time)
15 min	11.2	88
20 min	16.2	88
30 min	26.2	100

Table 4. Time savings based on the median over-forecast error for each cessation scheme with respect to the median over-forecast errors for the three 45WS wait times of 15, 20, and 30 min (Table 4) base on our storms. Positive values indicate a scheme that waits longer than the 45WS, while negative values represent schemes that wait less than the 45WS. The accuracy is presented for comparison with the scheme's time savings.

Scheme	Median Over-Error (min)	45WS Wait 15 min	45WS Wait 20 min	45WS Wait 30 min	Accuracy (Our Schemes)
99.5%	21.2	+10	+5	-5	100
95%	11.2	0	-5	-15	88
MZM LAG	11.6	+0.4	-4.6	-14.6	88
ETT	1.5	-9.7	-14.7	-24.7	81
SOR	2.9	-8.3	-13.3	-23.3	75
SSR	2.8	-8.4	-13.4	-23.4	75
CART	1.8	-9.4	-14.4	-24.4	56
ER	1.0	-10.2	-15.2	-25.2	44